Shifts in Depositional Environments as a Natural Response to Anthropogenic Alterations: Nakdong Estuary, South Korea

Joshua Williams[†], Timothy Dellapenna[†‡], Guan-hong Lee[§]

Department of Oceanography , Texas A&M University, College Station, Texas 77840

[‡] Department of Marine Sciences, Texas A&M University at Galveston, Galveston, Texas 77554

[§] Department of Oceanography , Inha University, Incheon, S. Korea 402-751

*Corresponding Author: jwilliams@ocean.tamu.edu, (409) 740-4746

Abstract:

The Nakdong Estuary, located within the coastal zone of Busan, South Korea, has been subjected to a series of engineered alterations typical of many eastern Asian estuaries. The construction of two estuarine dams (1934 and 1983) and numerous seawalls associated with land reclamation projects have altered the timing and flux of sediment, and resulted in three contrasting discharge energy regimes. Additionally, the impoundments have appreciably reduced the tidal prism. Consequently, vast geomorphologic changes have occurred including the development of five new barrier islands. In order to assess the impacts of these modifications, the dispersal and accumulation of sediment was evaluated utilizing ^{210}Pb and ^{137}Cs radioisotope geochronology of 6 cores. Average sediment accumulation rates range from 2.19 cm yr^{-1} adjacent to the first constructed dam, and were found to be as high as 6.55 cm yr^{-1} in the central portion of the estuary. These high rates are further supported by comparison of bathymetric survey data from 1985 to 2009. Laser diffraction grainsize analyses and X-radiographs revealed distinctive changes associated with dam construction, and correlation of events between cores conveys the episodic sedimentation corresponding to flood gate releases.

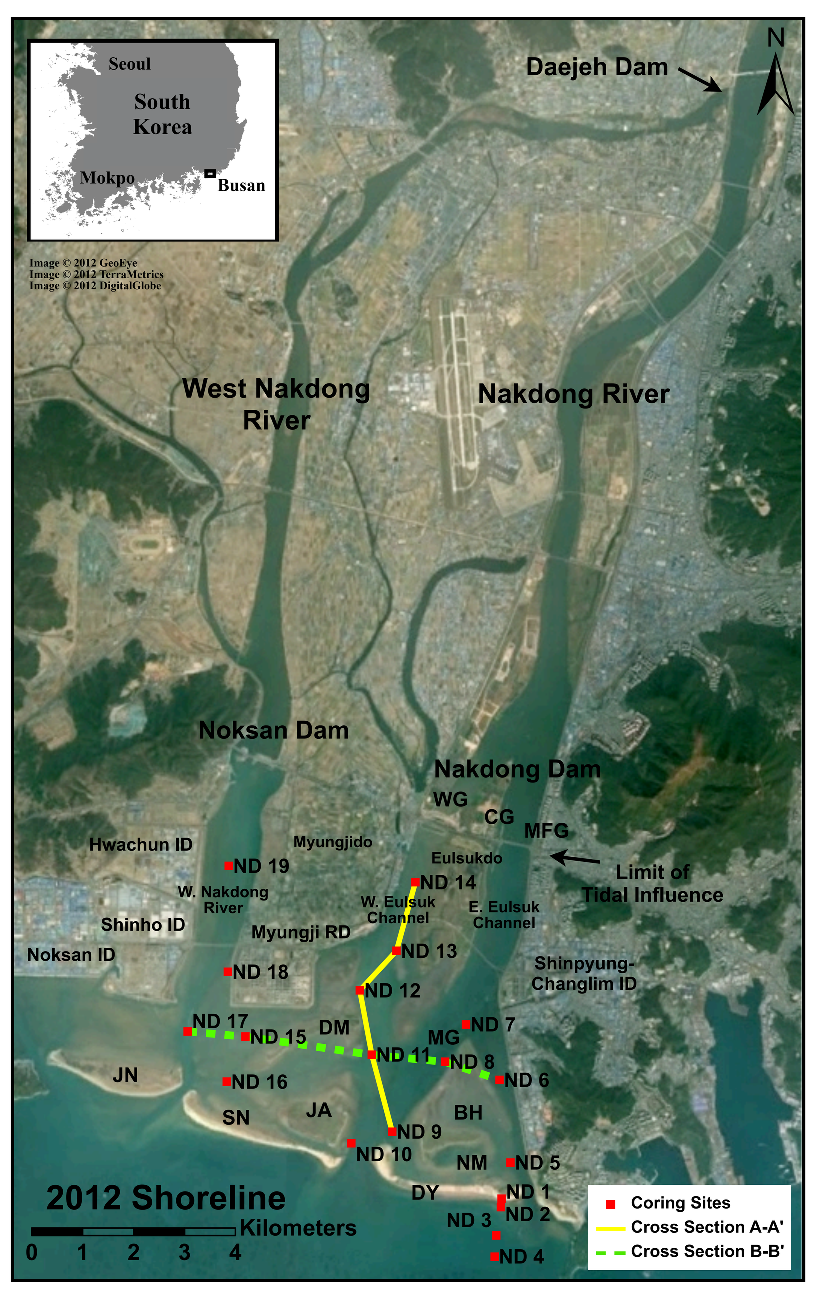

Fig. 1) Detailed study area map showing core sampling locations and cross sections. Noksan, Nakdong, and Daejeh Dam locations, channel names, barrier islands, and industrial (ID) and residential districts (RD) are indicated (WG=Western gate, CG=Control gate, MFG=Main floodgate, JN=Jinudo, DM=Daemadeung, JA=Jangjado, BH=Bakhabdeung, SN=Sinjado, DY=Doyodeung, NM=Namutsitdeung, and MG=Maenggeummeorideung).

Methods:

- 19 Vibracores of 7.6cm diameter were collected between Oct. 9-12, 2012.
- X-radiographs taken at 64 kV for 1.6 mAS with a Medison X-ray source and a Varian PaxScan® Amorphous Silicon Digital Imager.
- Grainsize analyses done via laser diffraction using a Malvern Mastersizer 2000 Particle Size Analyzer.
- ^{210}Pb activities were measured indirectly using ^{210}Po and counted by α-spectroscopy using a Canberra surface barrier detector.
- Activity of ^{137}Cs measured by gamma spectroscopy (662 keV) using a semi-planar intrinsic germanium detector coupled with CANBERRA DSA-1000 16K channel integrated multichannel analyzer.

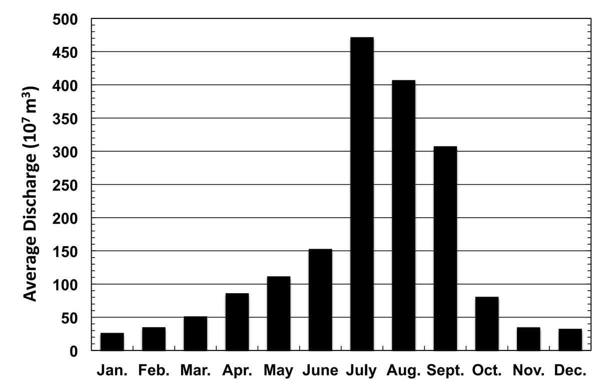

Fig. 2) Average monthly discharge from the Nakdong River Estuary Barrage for the period of Jan. 1990 - Aug. 2010.

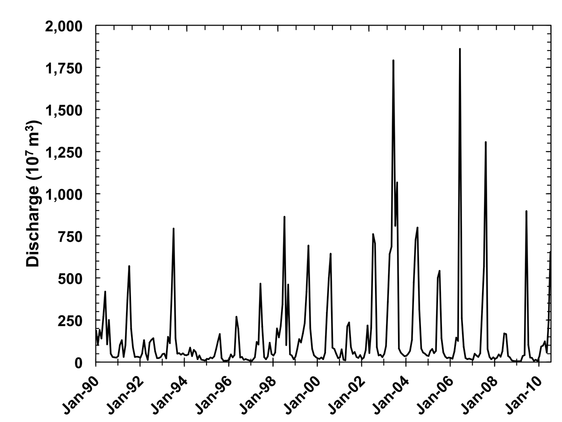

Fig. 3) Time series of total monthly discharge from the Nakdong River Estuary Barrage from Jan. 1990 - Aug. 2010.

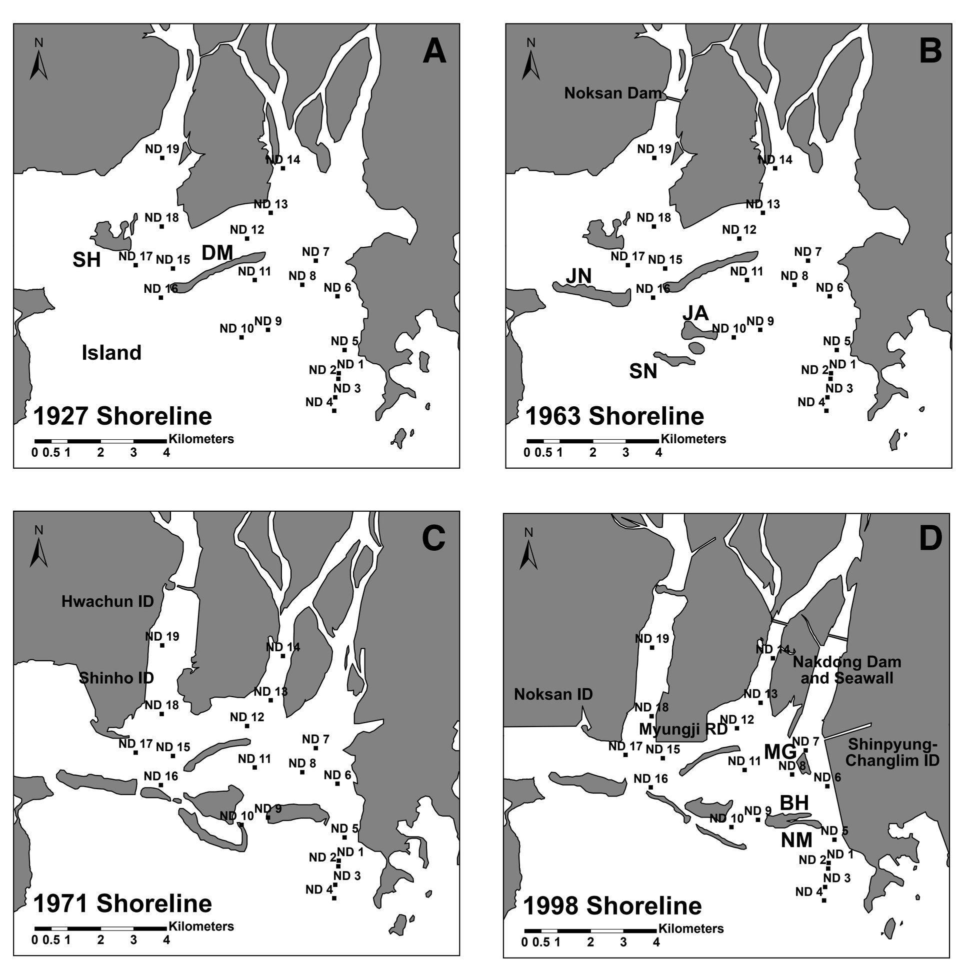

Fig. 4) Historical shoreline changes of the Nakdong Estuary compiled from KHOA marine charts. Construction and initiation of current islands occurring between publication dates of charts are indicated on the respective chart.

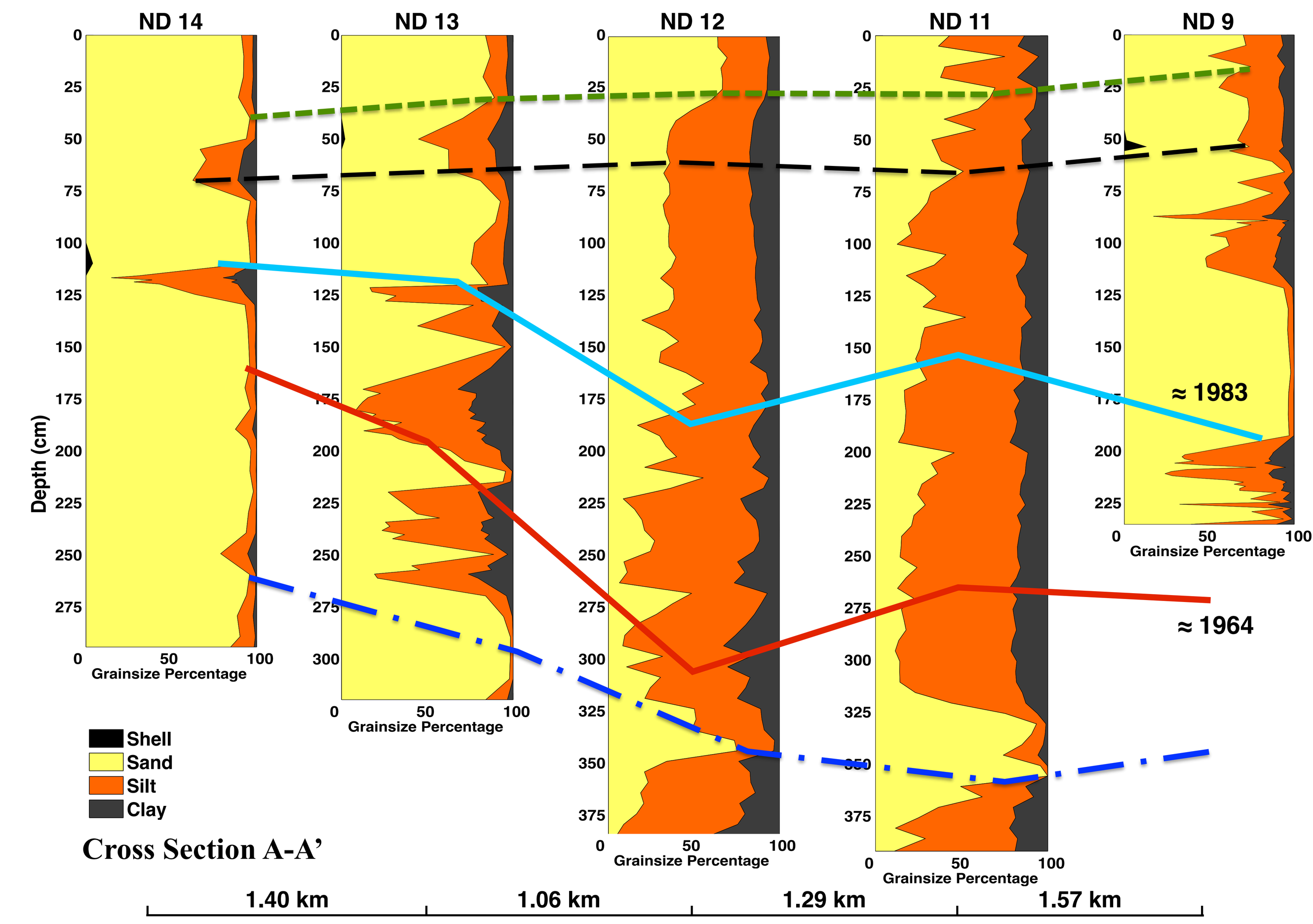

Fig. 6) Shore normal cross section through the W. Eulsuk Channel. Correlations are based on radiochemically derived data with minor depth change interpretations to respect grainsize profiles. Distances between cores are indicated and grainsize composition is represented as relative percentages.

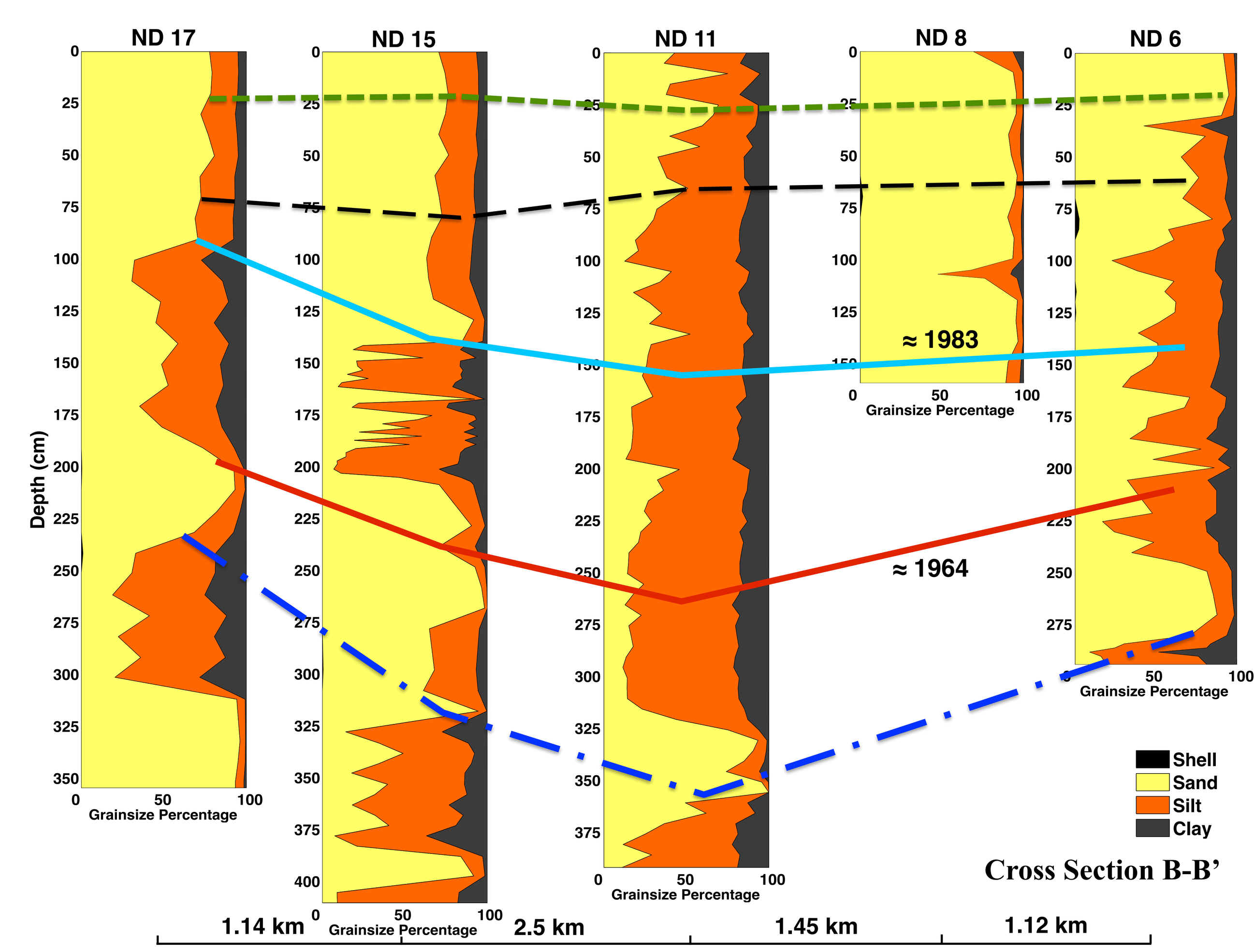

Fig. 7) Shore parallel cross section across the central portion of the Nakdong Estuary. Isochron identification is maintained from Cross Section A-A'.

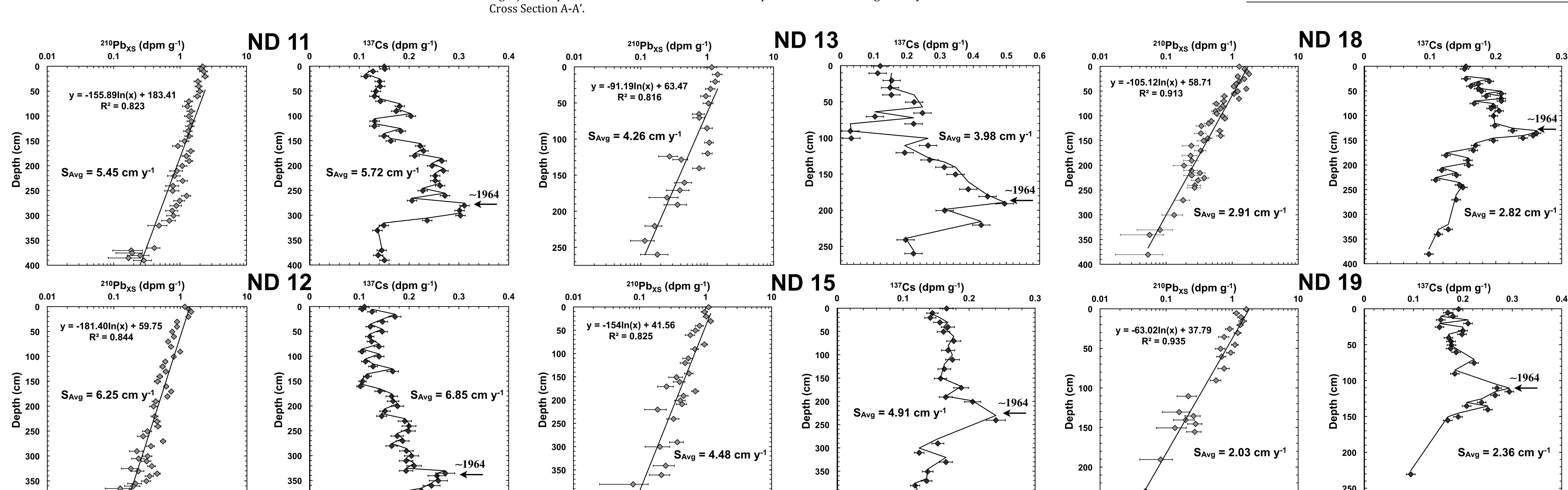

Fig. 5) Excess ^{210}Pb and ^{137}Cs profiles. Error bars for activity are indicated or occur within the range of the plot symbol. Regression line for $^{210}Pb_{xs}$ and respective average accumulation rates (S_{Avg}) are shown within plot. Note different depth scales depending on core.

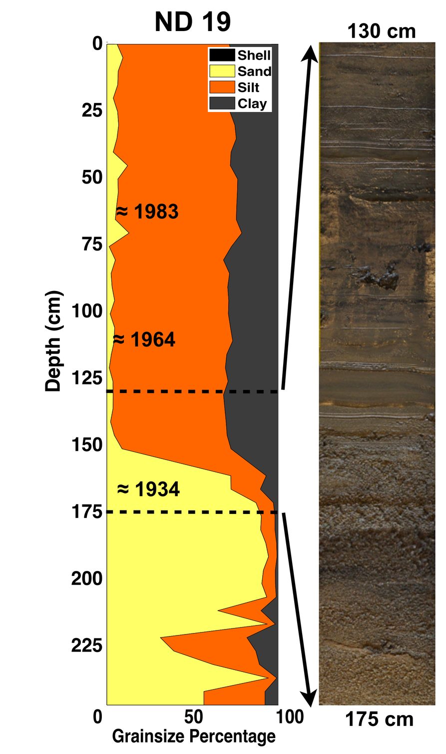

Fig. 8) Complete grainsize composition profile and core photograph for 130-175 cm section of core ND 19. A rapid increase in silt and clay percentage corresponds to the construction of the dam in 1934.

Table 1) Bathymetric survey data and accumulation rates for cores located a maximum 150 m from survey points.

Core	Dist. (m)	1985 Depth (m)	2009 Depth (m)	S_{Bath} (cm yr^{-1})
ND 11	112	-1.22	0.06	5.33
ND 12	148	-1.01	0.12	4.70
ND 17	63	-1.46	-0.70	3.18
ND 18	66	-0.61	0.03	2.67

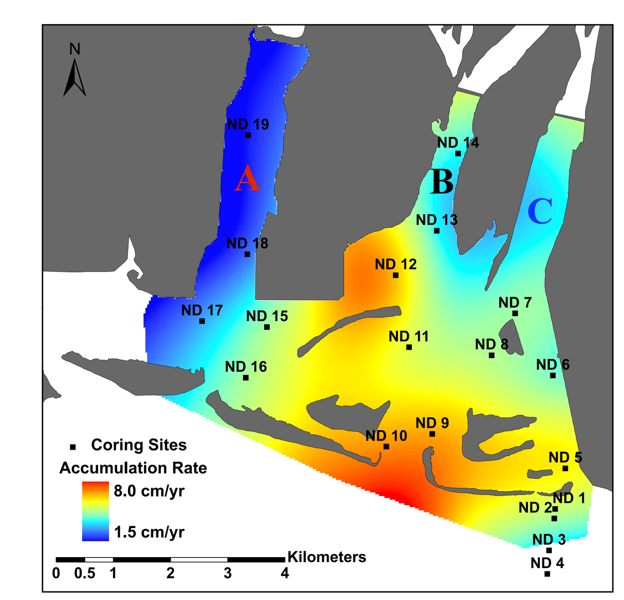

Fig. 10) Interpolated sediment accumulation rates. Known values are based on radioisotope analyses. Correlations of isochrons between cores were used to calculate unknown rates. Letters correspond to conceptual model in Fig. 11.

Table 2) Comparison of radioisotope accumulation rates derived from $^{210}Pb_{xs}$ and ^{137}Cs profiles. Averaged rates were used for correlation.

Core	^{210}Pb S_{Avg} (cm yr^{-1})	^{137}Cs S_{Avg} (cm yr^{-1})	Average (cm yr^{-1})
ND 11	5.45	5.72	5.59
ND 12	6.25	6.85	6.55
ND 13	4.26	3.98	4.12
ND 15	4.48	4.91	4.69
ND 18	2.91	2.82	2.86
ND 19	2.03	2.36	2.19

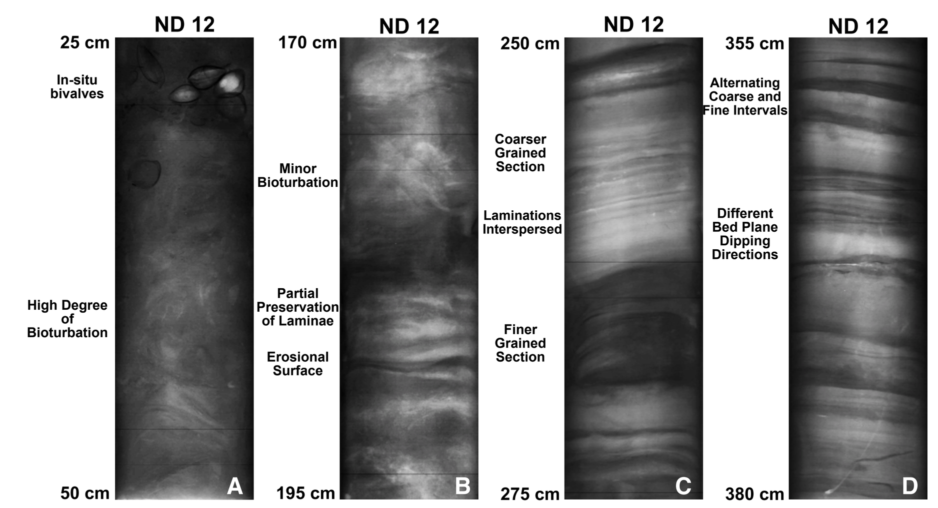

Fig. 9) Representative X-radiograph sections from core ND 12. Location within core and key features indicated.

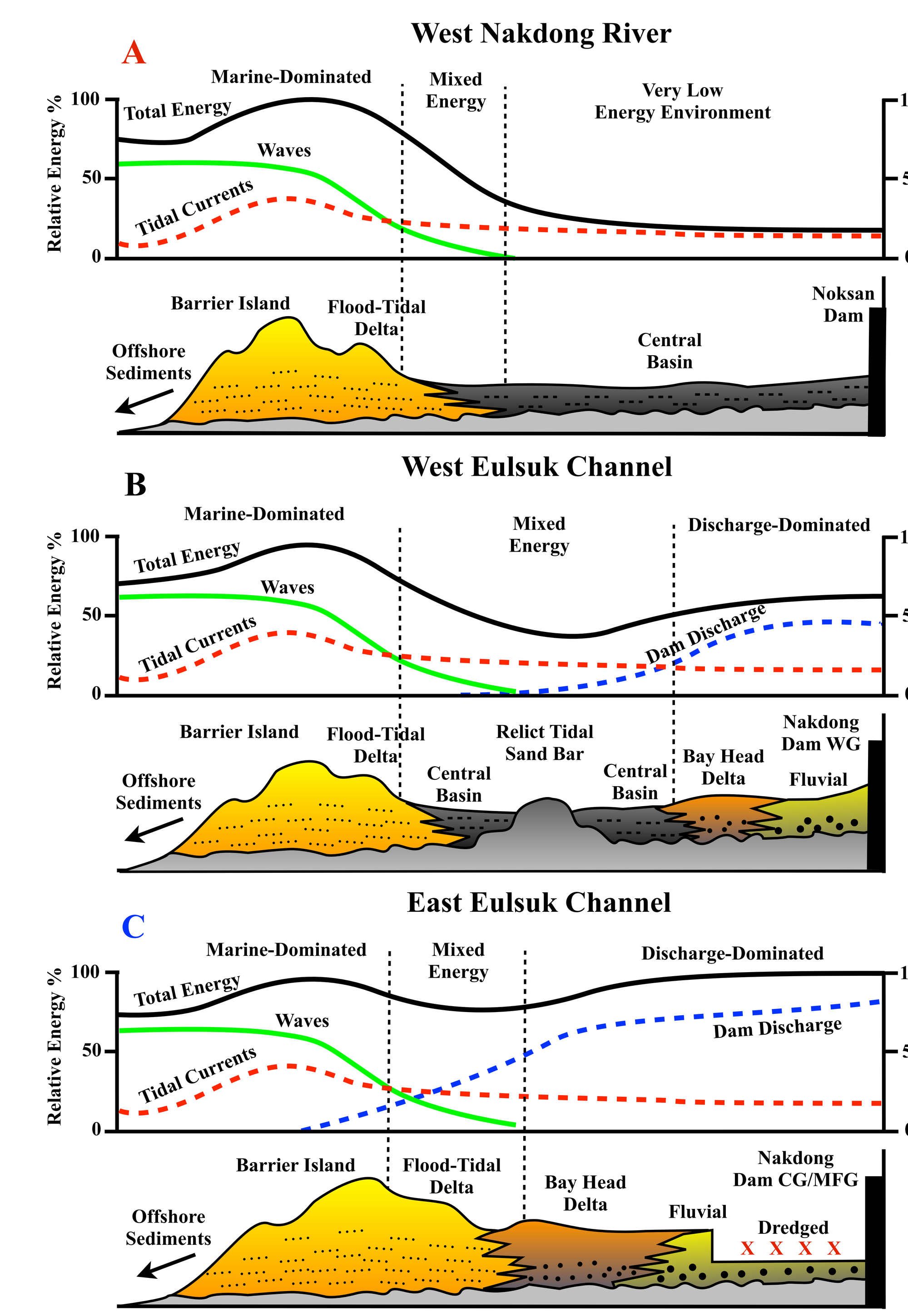

Fig. 11) Conceptual model for relative energy and facies distribution depending on dam discharge for a wave-dominated estuary. A) No discharge released B) Periodic (weekly to monthly), low energy discharge C) Consistent (daily to weekly), high energy discharge. Energy regimes are indicated as being either marine, mixed, or dam discharge dominated, and relative energy inputs are time averaged. Relative amounts of wave and tidal energy are assumed constant throughout the estuary.

Conclusions:

The construction of two estuarine dams and numerous seawalls have greatly modified the sediment transport dynamics of the Nakdong Estuary. These modifications have eliminated large areas of intertidal zone, and appreciably reduced the tidal prism and river discharge. Sediment flux to the estuary is restricted to floodgate releases which produce high flow velocities and episodic deposition.

The implications of these alterations are evident in a rapid geomorphologic shift from tide-influenced to wave-dominated. High sediment accumulation rates within the central estuary are due to a reduction in accommodation space in the upper estuary. Additional evidence for this reclassification occurs as a series of barrier islands that have developed post-dam construction accompanied by a redistribution of facies.

The increase in sediment trapping efficiency that has ensued resulting from extensive coastal construction provides the basis for reevaluating traditional facies models for unaltered estuaries. The observations made within this study have allowed the development of a conceptual model for facies distribution according to relative discharge energy of the adjacent floodgate.